

# PROBING THE EVOLUTION OF GALAXIES USING REDSHIFTED $H\alpha$ EMISSION

Paul P. van der Werf

*Leiden Observatory, Leiden, The Netherlands*

pvdwerf@strw.leidenuniv.nl

Alan F. M. Moorwood

*European Southern Observatory, Garching, Germany*

amoor@eso.org

Lin Yan

*SIRTF Science Center, Caltech, Pasadena, CA, U.S.A.*

lyan@ipac.caltech.edu

**Abstract** In this paper we review the present status and implications of  $H\alpha$  surveys at various redshifts. With the advent of sensitive wide-format near-infrared detectors on large telescopes, deep and extensive  $H\alpha$  surveys are now feasible to redshift  $z \sim 2.5$ . The cosmic star formation history can therefore be traced out to this redshift using  $H\alpha$  alone, avoiding complications arising from the comparison of different tracers at different redshifts. The  $H\alpha$  surveys to date confirm the rapid increase in luminosity density from  $z = 0$  out to  $z = 1$ , and show that this increase flattens off at higher redshifts, remaining approximately constant out to at least  $z \sim 2.2$ . We also discuss the prospects for determining the masses of high redshift galaxies based on emission lines. A set of high-quality  $H\alpha$  rotation curves of samples of disk galaxies at a number of different redshifts would allow a study of the evolution of the Tully-Fisher relation and address fundamental issues in disk galaxy formation. Such a program remains challenging even with present-day large telescopes.

**Keywords:** Galaxy evolution, disk galaxies

invited review, to appear in *Processings of the 2nd Hellenic Cosmology Workshop*, eds. M. Plionis et al. (Kluwer)

## 1. Introduction

When did the stellar populations of present-day galaxies form? This question is now beginning to be addressed by observations with modern telescopes in virtually all regions of the electromagnetic spectrum. Moderate redshift ( $z < 1$ ) surveys consistently indicate a cosmic star formation rate density (SFRD, the stellar mass formed per unit of time and per unit of comoving volume)  $\dot{\rho}_*$  that strongly increases with redshift out to  $z \sim 1$  (Hogg, 2001). The SFRD at  $z > 1$  is however a more hotly debated issue. Estimates based on surveys of Lyman break galaxies (e.g., Madau et al., 1996) sample rest-frame UV radiation and require a large and uncertain extinction correction (e.g., Pettini et al., 1998; Steidel et al., 1999). Submillimetre surveys, tracing reradiation by dust of absorbed starlight (e.g., Hughes et al., 1998; Blain et al., 1999) consistently indicate an even higher SFRD at these redshifts than even the extinction-corrected UV-determined values. As a result, the use of different star formation tracers at different redshifts complicates the reconstruction of the cosmic star formation history and it is therefore highly advantageous to use the same star formation tracer at all redshifts. The  $H\alpha$  line is the natural choice for this tracer, since with the development of large area, high quality near-infrared arrays, this line can now be observed in the  $J$ ,  $H$  and  $K$ -bands, where redshifts of approximately 1, 1.5 and 2.2 respectively, are accessible.

Traditionally, emission-line surveys for high- $z$  star forming galaxies have targeted the  $Ly\alpha$  line, which moves into the optical regime for  $z = 1.9 - 7.0$ . However, since  $Ly\alpha$  is resonantly scattered, even very small quantities of dust will effectively suppress the line (Charlot & Fall 1991, 1993; Chen and Neufeld, 1994). Spectroscopic observations of star forming  $z > 3$  Lyman break galaxies (Steidel et al., 1996) confirm that  $Ly\alpha$  is not a good tracer of star formation in high- $z$  galaxies. These galaxies form stars at rates of  $\sim 10 M_\odot \text{ yr}^{-1}$  as derived from their restframe UV properties (uncorrected for extinction), but  $Ly\alpha$  is absent (or in *absorption*) in more than 50% of the cases, while in most of the remaining objects the line is faint. Thus, while  $Ly\alpha$  searches can be used to find high- $z$  star forming galaxies (e.g., Hu and McMahon, 1996; Hu et al., 1998; Cowie and Hu, 1998; Manning et al., 2000; Stern et al., 2000; Kudritzki et al., 2000; Rhoads et al., 2000; Steidel et al., 2000), such surveys cannot provide reliable star formation rates (SFRs) for the galaxies that are detected.

This complication is avoided by searching for  $H\alpha$  emission in stead of  $Ly\alpha$ . The  $H\alpha$  line is not resonantly scattered and thus much less sensitive to the effects of small amounts of dust. In addition, the broad-

band extinction at  $H\alpha$  (6563 Å) is much less than that at  $Ly\alpha$  (1215 Å) ( $A_{Ly\alpha}/A_{H\alpha} = 4.28$  for the extinction curve used by Cardelli et al., 1989). Although the extinction at the wavelength of  $H\alpha$  is still large in starburst galaxies, the typical  $H\alpha$  extinction in local spiral galaxies is only  $1^{m1}$  (Kennicutt, 1983 and references therein). A recent comparison of star formation tracers (including stellar continuum emission as well as nebular lines) confirms that  $H\alpha$  is the most robust star formation tracer, and can give results accurate to within a factor of 2 to 3 when combined with other tracers, even if the  $H\alpha/[N II]$  blend is not resolved (Charlot and Longhetti, 2001). In contrast, the also widely used  $[O II]$  line at 3727 Å is a more uncertain star formation tracer by a full order of magnitude, because of uncertainties in excitation, metallicity and reddening. The SFR derived from  $H\alpha$  also correlates well with that estimated from the UV (Bell and Kennicutt, 2001). The systematically higher SFR derived from  $H\alpha$  (by a factor of 1.5 in relatively luminous galaxies) simply reflects the difference in extinction between the optical and UV regimes.

In this paper we first review the current status of  $H\alpha$  surveys from  $z = 0$  out to the highest redshifts where such surveys have been performed to date. Since we only consider  $H\alpha$ , this analysis should be free of uncertainties introduced by using different tracers at different redshifts. Uncertainties in the conversion of  $H\alpha$  luminosity into SFR rate can be avoided by quoting the  $H\alpha$  luminosity density, which can be derived directly by integrating the  $H\alpha$  luminosity function.

In the second part of this review we address the use of  $H\alpha$  for studying the kinematics of high- $z$  galaxies. While the SFRD is expressed as a time derivative of comoving *mass* density, the various ways of determining SFRD do not involve the measurement of mass but of light. However, the stars producing most of the light contain very little mass, while the stars containing most of the mass produce little light, for a typical initial mass function (IMF). As a result, calculating the *total* SFR from a measurement of light (regardless of whether this is rest-frame ultraviolet light, nebular line emission, or emission from dust) always involves the uncertain step of assuming an IMF. While systematic errors in the analysis can be mitigated by ensuring that always the same IMF is *assumed*, the universality of the IMF is still an assumption and a very debatable issue. The most direct way of avoiding this complication is by making a dynamical mass measurement. Spectral line measurements offer this possibility, provided the kinematic pattern is dominated by gravitational motion. For this reason,  $Ly\alpha$  kinematics is normally not useful since  $Ly\alpha$  line profiles are often affected by nongravitational motions such as outflows. Emission line kinematics can be assumed to be

dominated by gravitational motion if a characteristic pattern such as a rotation curve is observed. Even then, one must be wary of excitation effects, since lines such as [O III] 5007 Å possibly sample only the inner parts of a galaxy, and may not reveal the full amplitude of the rotation curve. Again, using H $\alpha$  is the best way for avoiding such biases.

Dynamical measurements of this type have the potential for probing the evolution of the Tully-Fisher (TF) luminosity-line width relation out to  $z \sim 2.5$ . This issue is directly related to the physics of disk galaxy formation. One model for the origin of the TF relation argues that the dark halo is the sole factor determining the disk properties (and therefore the TF relation), since the outer region of disks, where the rotation curves are flat, are dynamically dominated by the dark halo. Models based on this observation predict rapid evolution of the TF relation (Mo et al., 1998). On the other hand, it has been proposed that the TF relation is entirely the result of star formation self-regulation in the disk interstellar medium and has nothing to do with the halo at all (Silk, 1997). A set of high-quality H $\alpha$  rotation curves of disk galaxies at a number of different redshifts is needed to settle this fundamental issue from an observational point of view. First results and prospects in this challenging field are reviewed in Sect. 3.

Unless noted otherwise, in this review, all quantities that are dependent on cosmology are quoted for a universe with  $(h, \Omega_M, \Omega_\Lambda) = (0.5, 0.5, 0.0)$ , where the Hubble constant is  $H_0 = 100 h \text{ km s}^{-1} \text{ Mpc}^{-1}$  and  $\Omega_M$  and  $\Omega_\Lambda$  are the present-day density parameters of matter and of the cosmological constant, respectively. Where necessary, results originally quoted for other cosmologies have been tacitly converted.

## 2. The cosmic star formation history derived from H $\alpha$ surveys

### 2.1. Surveys and strategies

Observationally, the task of measuring the SFRD at a particular redshift from H $\alpha$  consists of determining the H $\alpha$  luminosity function, which is parametrized (Schechter, 1976) as

$$\phi(L) dL = \phi^* (L/L^*)^\alpha e^{-L/L^*} d(L/L^*) \quad (1)$$

and gives the number density (per  $\text{Mpc}^3$ ) of galaxies with luminosities between  $L$  and  $L + dL$ . For cosmological applications, *comoving* number densities (i.e., number of galaxies per comoving  $\text{Mpc}^3$ ) are computed. In practice, the number density of galaxies is binned per 0.4 interval in

$\log L$ , which can be related to the standard form by

$$\Phi(\log L) \frac{d \log L}{0.4} = \phi(L) dL. \quad (2)$$

The total luminosity density is found by integrating the luminosity function over all luminosities:

$$\rho_L = \int L \phi(L) dL = \phi^* L^* \Gamma(2 + \alpha), \quad (3)$$

where  $\Gamma$  denotes the gamma function. For a determination of the total luminosity density it is therefore sufficient to determine the three parameters  $\phi^*$ ,  $L^*$  and  $\alpha$  of the luminosity function. Note that the integrated luminosity density is dominated by low-luminosity objects if  $\alpha$  approaches  $-2$ .

Surveys for emission line objects can be of three types (cf., Djorgovski, 1992). Slitless spectroscopic surveys sample large volumes of space but can only achieve interesting depths when carried out from space. Ground-based surveys can be either serendipitous long-slit surveys (covering a large redshift range but a very limited solid angle) or narrow-band surveys (sampling a large area but in a very narrow redshift interval). Since the background in the near-IR windows shortward of about  $2.2 \mu\text{m}$  is dominated by OH emission lines, the narrow-band survey technique is the ideal approach in this spectral region for ground-based observations. This technique involves deep imaging in a suitable narrow-band filter, complemented with broad-band imaging; sources with excess flux in the narrow-band filter are emission line candidates in a redshift interval determined by the narrow-band filter passband (this strategy has been analyzed in detail by Mannucci and Beckwith, 1995). Narrow-band surveys of  $H\alpha$  emission at  $z > 2$  were initially unsuccessful (Thompson et al., 1994; Pahre and Djorgovski, 1995; Bunker et al., 1995; Collins et al., 1996; Thompson et al., 1996) due to lack of depth and/or coverage (with the exception of one object at  $z = 2.43$  reported by Beckwith et al., 1998). In contrast, more extensive  $H\alpha$  surveys targeted at volumes containing known damped  $\text{Ly}\alpha$  and metal-line absorbers, quasars and radio galaxies resulted in the identification of a significant number of candidate objects (Mannucci et al., 1998; Teplitz et al., 1998; van der Werf et al., 2000). However, since none of these surveys has been successfully followed up with spectroscopic confirmation, these results must so far be considered tentative. More fundamentally, since these were *targeted* surveys, centred at particular “marker” objects of known redshift, they are most likely biased to overdense regions and cannot be used to derive a star formation rate density that is valid for the universe on global scales.

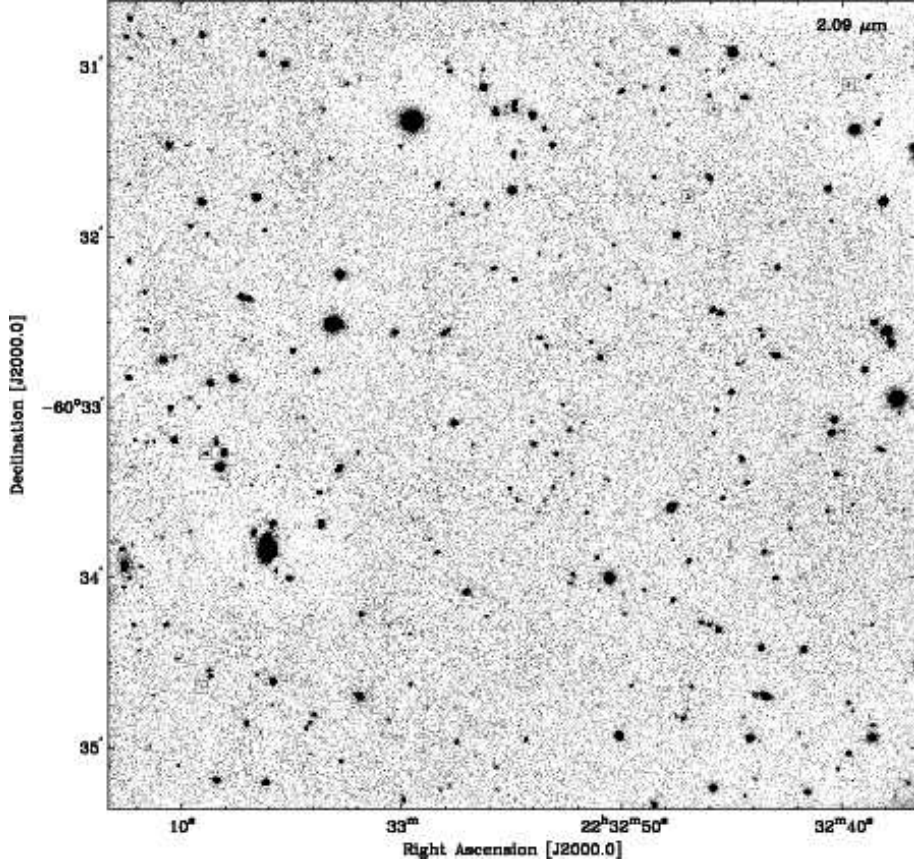


*Figure 1a.* Narrow-band image at  $2.09 \mu\text{m}$  centred on the HDFS WFPC2 field. The field size is  $5' \times 5'$  with North at the top and East to the left. The squares identify spectroscopically confirmed emission-line sources (from Moorwood et al., 2000).

## 2.2. Blank field $\text{H}\alpha$ surveys

**2.2.1 Surveys at  $z \lesssim 1$ .** The  $\text{H}\alpha$  luminosity density of the local ( $z < 0.045$ ) universe has been determined from the Universidad Complutense de Madrid objective prism survey (Gallego et al., 1995). At somewhat higher redshift, the  $\text{H}\alpha$  luminosity density derived from a  $\langle z \rangle \sim 0.2$  sample taken from the  $I$ -band selected Canada France Redshift Survey (CFRS) is about a factor of 2 higher (Tresse and Maddox, 1998). A small survey of 13 CFRS galaxies at  $z \approx 0.9$  produced an  $\text{H}\alpha$  luminosity density approximately 10 times higher than that at  $z \sim 0$

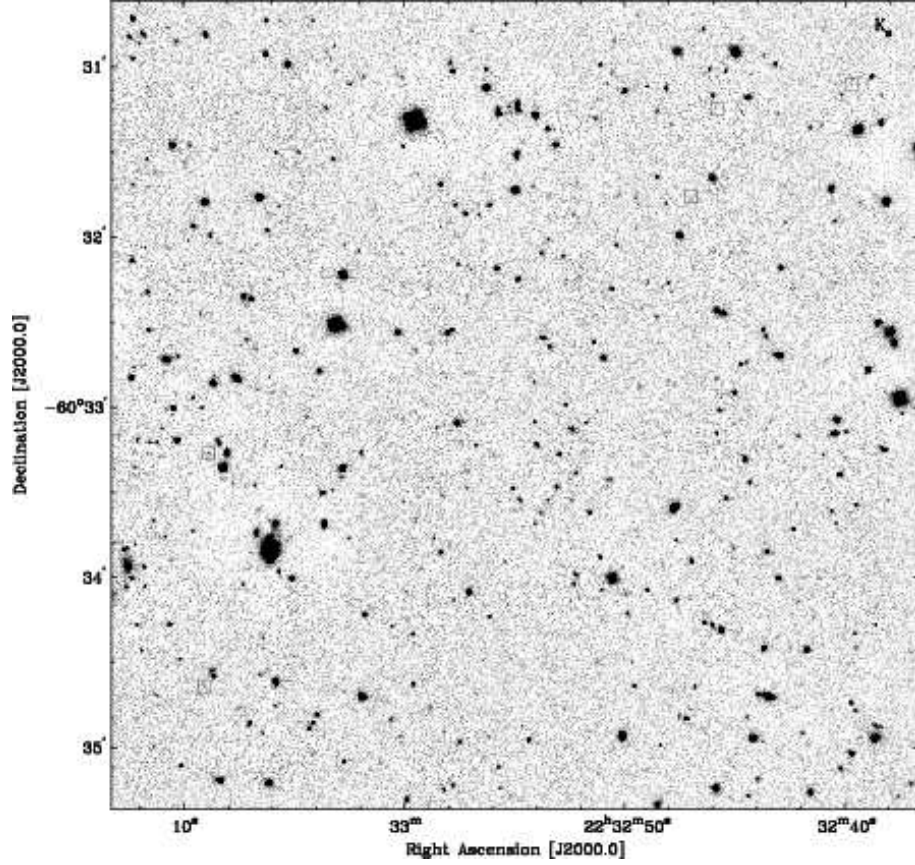


Figure 1b. Broad-band  $K_s$  image corresponding to the  $2.09\ \mu\text{m}$  narrow-band image of the HDFs WFPC2 field (from Moorwood et al., 2000).

(Glazebrook et al., 1999). All of these results include a small (approximately 1 magnitude) correction for extinction, and a correction for the effects of the  $[\text{N II}]$  lines on the derived  $H\alpha$  flux. The magnitude of this increase is in excellent agreement with the increase in cosmic luminosity density measured in the rest-frame ultraviolet (Lilly et al., 1996) and in radio continuum emission (Haarsma et al., 2000). The redshift region out to  $z \sim 1$  is thus characterized by a strong increase in luminosity density with lookback-time. While the precise values of the corresponding star formation rate densities are uncertain due to the complications discussed in Sect. 1, the increase out to  $z \sim 1$ , when measured in one par-

ticular tracer, is now well documented and is quantitatively consistent between various different tracers (Hogg, 2001).

It should be emphasized that existing  $H\alpha$  surveys at  $z \lesssim 1$  are limited in both width (leading to poor statistics, especially at the high luminosity end) and depth (leading to a poor determination of the faint-end slope of the luminosity function). Indeed, a recent deeper narrow-band survey for  $H\alpha$  at redshifts of approximately 0.08, 0.2 and 0.4 (Jones and Bland-Hawthorn, 2001) suggests the need for an upward revision of the local  $H\alpha$  luminosity density, mainly as a result of a higher detection rate of faint galaxies. This result is in agreement with an analysis of the KPNO International Spectroscopic Survey (Gronwall, 1999), based on 1126  $H\alpha$  emitters at  $z < 0.085$  detected using the objective prism technique.

**2.2.2 Surveys at  $1 \lesssim z \lesssim 2$ .** The redshift range between redshifts 1 and 2 is of fundamental interest since it is in this range that the cosmic star formation history starts to turn over from a fairly high level of star formation rate density (perhaps to first order constant with redshift at  $z \gtrsim 1$ ) into the rapid decrease discussed in the previous section. The shape, origin, and redshift of this turnover are not well known. This lack of knowledge is partly explained by the lack of suitable redshift tracers in the optical region for redshifts between 1 and 2. In addition, at  $z \gtrsim 1$  the  $H\alpha$  line has moved into the near-infrared regime and sensitive large-format near-infrared cameras and spectrographs at large telescopes have only recently become available.

The most important  $H\alpha$  surveys at  $1 \lesssim z \lesssim 2$  to date are the two slitless grism surveys carried out with NICMOS on the Hubble Space Telescope. The first of these surveys (McCarthy et al., 1999) covered approximately  $64\text{ arcmin}^2$  and yielded an  $H\alpha$  luminosity function (Yan et al., 1999) with  $L^*(H\alpha)$  exceeding the  $z = 0$  value (Gallego et al., 1995) by a factor of 7, implying significant luminosity evolution. The second survey (Hopkins et al., 2000), covered only  $4.4\text{ arcmin}^2$  but extended the  $H\alpha$  luminosity function towards fluxes fainter by a factor of 2, pinning down the faint-end slope of the luminosity function at  $\alpha = -1.6$ . In total these surveys produced 70  $H\alpha$  emitters between  $z = 0.7$  and 1.9. A significant fraction of these have been confirmed as  $H\alpha$  emitters by spectroscopy of other emission lines. Since the two grism surveys define the  $H\alpha$  luminosity function at  $\langle z \rangle \sim 1.3$  over a significant range in luminosity, the implied  $H\alpha$  luminosity density is well-determined. The resulting value is  $3.6 \cdot 10^6 \text{ L}_\odot \text{ Mpc}^{-3}$ , without any correction for extinction. It is remarkable that this value is 15% *smaller* than the  $z = 0.9$  value (Glazebrook

et al., 1999), and the steep rise in luminosity density from  $z = 0$  to 1 therefore appears to flatten off at  $z > 1$ .

**2.2.3 Surveys at  $z > 2$ .** The highest redshift survey for  $H\alpha$  emitters used the SOFI near-infrared camera on the ESO New Technology Telescope to target a  $100\text{''}$  area in the region of the Hubble Deep Field South (HDFS), in a narrow ( $\Delta z \approx 0.04$ ) redshift interval at  $z \approx 2.2$ , using the narrow-band imaging technique (Moorwood et al., 2000). This redshift interval was chosen because it redshifts  $H\alpha$  to  $2.09\text{ }\mu\text{m}$ , which is a spectral region relatively free of bright OH lines and not strongly affected by the thermal background that becomes dominant at somewhat longer wavelengths. The importance of this survey lies in the fact that it is the first successful blank-field survey of this type and at this redshift, and the only one with substantial spectroscopic confirmation. One field from this survey is shown in Fig. 1. It reveals 5 emission line objects, all of which are spectroscopically confirmed. A set of confirmation spectra, obtained with ISAAC at the ESO Very Large Telescope, is shown in Fig. 2. The number of detections from this survey matches precisely the number expected under the assumption that the  $H\alpha$  luminosity function at  $z \sim 2.2$  is identical to that at  $z \sim 1.3$ . The number density of  $H\alpha$  emitters at  $z \sim 2.2$  is also comparable to that of Lyman break galaxies with similar SFRs at  $z = 3.0 - 3.5$  (Steidel et al., 1996). These results provide further evidence for a constant SFRD at  $z > 1$ .

### 2.3. The evolution of the $H\alpha$ luminosity density and star formation in galaxies

Comparison of the luminosity functions at  $z \sim 0$  (Gallego et al., 1995) and  $z \sim 1.3$  (Yan et al., 1999) and higher shows that both luminosity evolution and density evolution are implied. However, luminosity evolution dominates (a factor 7 increase in  $L^*$  from  $z = 0$  to  $z = 1.3$  compared to a factor 2.6 increase in  $\phi^*$ ). Indeed, in the  $z \sim 2.2$  sample the implied SFRs are 20 to  $35\text{ M}_\odot\text{ yr}^{-1}$  (for the  $H\alpha$ /SFR conversion factor of Kennicutt, 1998, which is appropriate for continuous star formation and a Salpeter IMF, at solar metallicity). These values are significantly higher than in typical nearby galaxies, but lower than in extreme starburst galaxies, such as are found in submillimetre surveys (e.g., Ivison et al., 2000). This result suggests that, while the submillimetre measurements select extreme starburst objects which may plausibly be identified with the formation of present-day spheroids, the  $H\alpha$  measurements select a less extreme mode of star formation. It may then be speculated that the

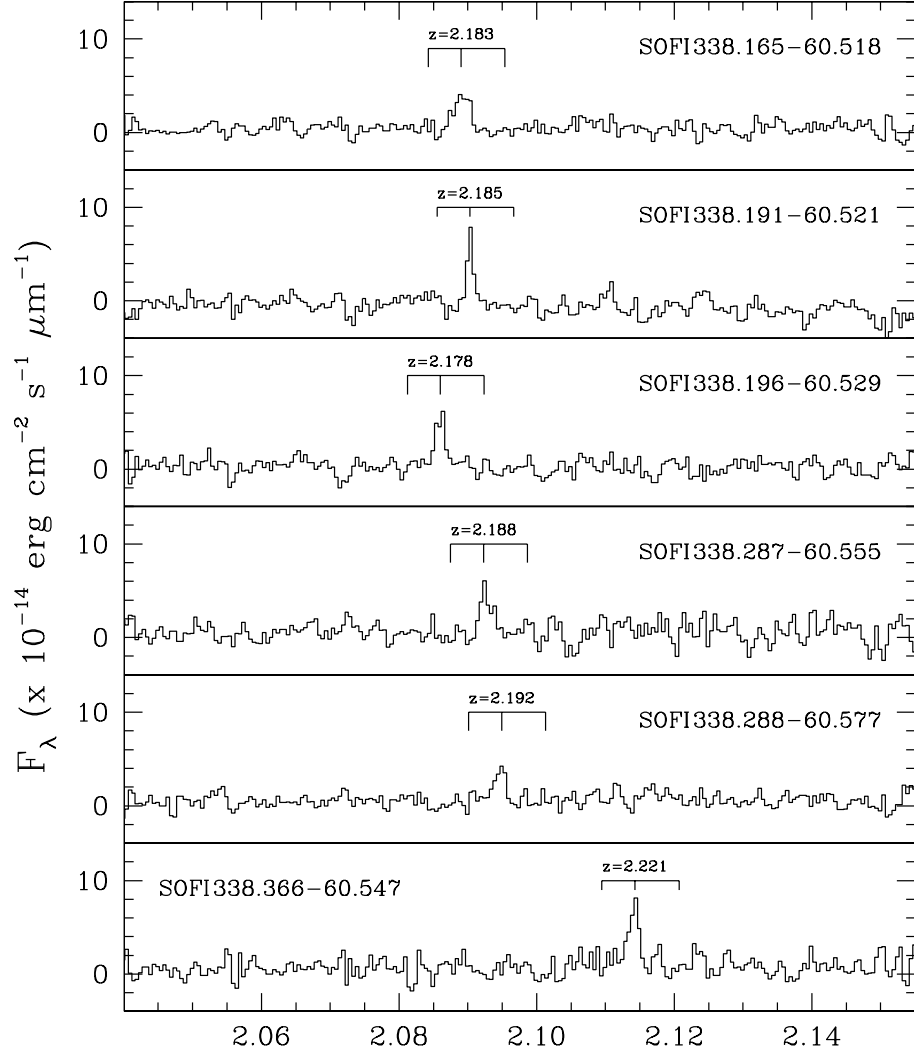


Figure 2. ISAAC spectra of emission line galaxies from the HDFS narrow-band imaging survey (Moorwood et al., 2000). The markers under the redshift labels show the expected wavelengths of the [N II] (6548 and 6584 Å) lines assuming the detected line is H $\alpha$ .

H $\alpha$  measurements trace the buildup of disks. Dynamical measurement (cf., Sect. 3) may shed light on this hypothesis.

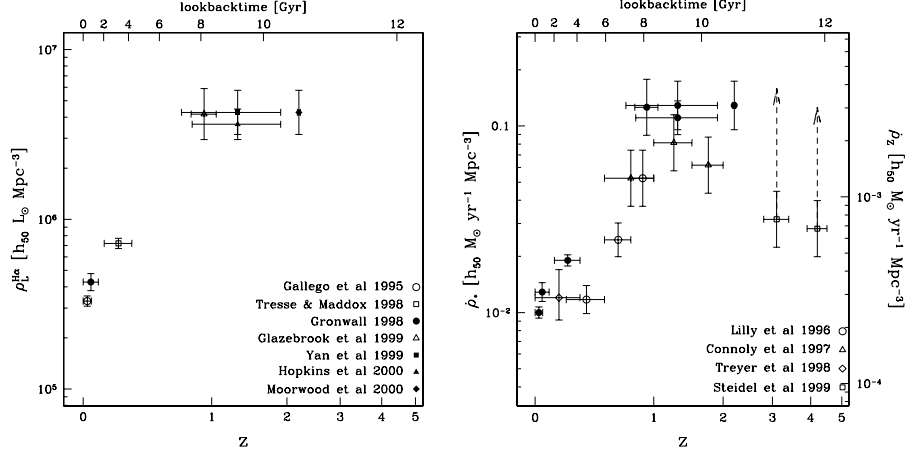


Figure 3. The evolution of the cosmic  $H\alpha$  luminosity density (lefthand panel) and SFRD (righthand panel, calculated using the  $H\alpha$ /SFR conversion factor of Kennicutt, 1998). In the lefthand panel, open symbols denote measurements that include an extinction correction based on the Balmer decrement. In the right-hand panel, filled symbols denote the  $H\alpha$ -based measurements while open symbols are based on rest-frame UV radiation; the arrows on the 2 high-redshift points in this panel indicate the magnitude of the estimated extinction correction. In the righthand panel, the righthand vertical axis denotes metal production rate density, which is less sensitive to the assumed IMF than star formation rate density (Madau et al., 1996).

The evolution of the  $H\alpha$  luminosity density and the implied SFRD history are summarized in Fig. 3. The  $H\alpha$  results give a consistent picture of evolution out to  $z \sim 2.2$ . Without extinction corrections, the  $H\alpha$  surveys imply higher SFRDs than the UV-based surveys, but the discrepancy is typically only a factor of 2 (Fig. 3). It is interesting that the extinction corrections proposed for Lyman break galaxies at higher redshifts lead to an SFRD very similar to that implied by the  $H\alpha$  surveys (see Fig. 3); it should be noted however, that these corrections are not very certain.

### 3. Dynamical mass measurements at high redshifts using $H\alpha$

The low-redshift TF relation derived from  $H\alpha$  rotation curves is well-defined (Courteau, 1997). Attempts to detect evolution in the zero-point of the TF relation using  $H\alpha$  measurements of higher redshift samples are so far inconclusive: while  $H\alpha$  rotation curves out to  $z \sim 1$  implied only

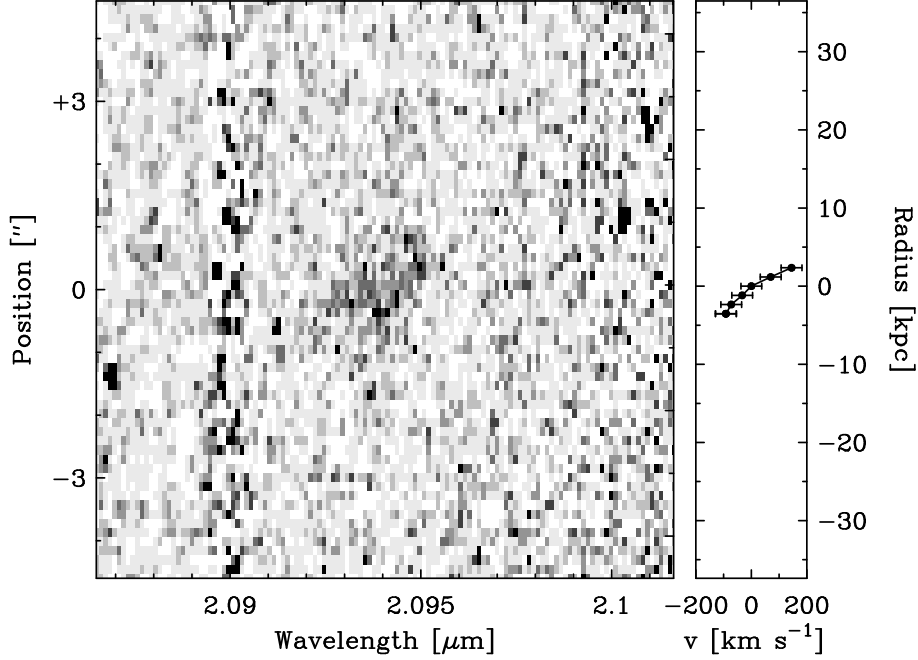


Figure 4. Long-slit  $H\alpha$  spectrum of a galaxy at  $z \sim 2.2$  showing the signature of ordered rotation (left panel); the implied rotation curve is shown in the right-hand panel (Moorwood et al., 2000).

about  $0^m4$  evolution in  $B$  (Vogt et al., 1996, 1997), a study of  $[O\text{II}]$  rotation curves at  $\langle z \rangle = 0.35$  suggested luminosity evolution by  $1.5 - 2$  magnitudes in  $B$  (Simard and Pritchett, 1998). These results may be reconciled if in the  $[O\text{II}]$  data the rotation curves are not sampled all the way out to the flat part. The discrepancy underlines the need for deep uniform  $H\alpha$  rotation curves for projects of this type.

Since the effects of evolution should be largest at high redshift,  $H\alpha$  dynamics is particularly important for the most distant galaxies from the surveys described in Sect. 2. One of the galaxies from the  $z \sim 2.2$  SOFI/ISAAC survey (Moorwood et al., 2000) actually shows a tilt in the 2-dimensional spectrum (taken along a position angle within  $10^\circ$  of the major axis of the galaxy) indicating ordered rotation (Fig. 4). With the short integration time of 1 hour only the central portion of the rotation curve is seen, so that only a lower limit to the total line width can be determined. The resulting peak-to-peak velocity width is  $247 \pm 30 \text{ km s}^{-1}$ , which increases to  $275 \pm 30 \text{ km s}^{-1}$  after applying a

correction for inclination. Thus a rotational velocity of  $138 \pm 15 \text{ km s}^{-1}$  is implied at a radius of 3 kpc. These parameters are comparable to those of local disk galaxies which have rotation curves flattening at velocities between 100 and 300  $\text{km s}^{-1}$  at radii of 1 to 5 kpc. It is therefore evident that well-developed, relatively massive systems already occur at  $z \sim 2.2$ . More interestingly, with a rest-frame absolute  $B$  magnitude  $M_B = -22.4$  this object lies about 3 magnitudes above the local  $B$ -band TF-relation. This conclusion can only be avoided if the full rotation curves extends to over 1000  $\text{km s}^{-1}$  and only flattens at a radius larger than 12 kpc which would imply an *extremely* massive galaxy and is therefore unlikely.

#### 4. Conclusions and outlook

Surveys of  $H\alpha$  emission are now beginning to probe the cosmic star formation history out to  $z \sim 2.2$  in a meaningful manner. However, this field is still in a very early stage of development. A fundamental problem is that the samples are small, leading to uncertainty in the derived luminosity function. This is best illustrated by the fact that even at  $z \sim 0$ , where the available samples are largest, significant discrepancies remain (cf., Sect. 2.2.1). Great progress in determining the  $H\alpha$  luminosity density at low redshifts should be made as a result of the Sloan Digital Sky Survey and associated follow-up. At higher redshifts, the VIRMOS survey at the ESO Very Large Telescope should provide a census out to redshifts beyond 1. Redshifts  $z > 2$  bring  $H\alpha$  into the  $K$ -band and an efficient survey would require a cryogenic multi-object spectrograph. At  $z > 2.5$   $H\alpha$  shifts into the thermal infrared and the Next Generation Space Telescope will provide the first opportunity for deep  $H\alpha$  measurements at these redshifts.

As important as the composition of good samples is a good estimate of the extinction.  $H\alpha$  extinctions can be determined from the Balmer decrement, and should be feasible for most galaxies where  $H\alpha$  can be detected. Furthermore, for a reliable determination of star formation based on  $H\alpha$ , other spectral features should also be observed (Charlot and Longhetti, 2001).

First results on  $H\alpha$  kinematics at high redshift demonstrate the feasibility of determining rotation curves of high- $z$  galaxies with present-day instrumentation. Compiling a sample of high-quality  $H\alpha$  rotation curves at a number of redshifts out to  $z \sim 2.2$  will be extremely valuable for our understanding of the disk galaxy formation and the origin of the Tully-Fisher relation. Such a project should ideally make use of the multiplexing capabilities of future cryogenic multi-integral-field-unit near-infrared spectrographs. However, a first sample of well-measured rotation curves

out to  $z \sim 2.2$  can already be built up with deep near-infrared  $H\alpha$  spectroscopy of galaxies from the existing samples. This is within reach with present-day near-infrared spectrographs on large telescopes.

## Acknowledgments

PvdW would like to thank the organisers for a very enjoyable meeting. It was an honour to be able to discuss the cosmos in the same city where man first realized that nature lends itself to analysis by the human mind. Special thanks go to Padelis Papadopoulos and his family for excellent Greek hospitality.

## References

- Beckwith, S. W. V., Thompson, D., Mannucci, F., and Djorgovski, S. G. (1998). An infrared emission-line galaxy at  $z = 2.43$ . *ApJ*, 504:107.
- Bell, E. F. and Kennicutt, R. C. (2001). A comparison of ultraviolet imaging telescope far-ultraviolet and  $H\alpha$  star formation rates. *ApJ*, 548:681.
- Blain, A. W., Smail, I., Ivison, R. J., and Kneib, J.-P. (1999). The history of star formation in dusty galaxies. *MNRAS*, 303:423.
- Bunker, A. J., Warren, S. J., Hewett, P. C., and Clements, D. L. (1995). On near-infrared  $H\alpha$  searches for high-redshift galaxies. *MNRAS*, 273:513.
- Cardelli, J. A., Clayton, G. C., and Mathis, J. S. (1989). The relationship between infrared, optical, and ultraviolet extinction. *ApJ*, 345:245.
- Charlot, S. and Fall, S. M. (1991). Attenuation of Lyman-alpha emission by dust in damped Lyman-alpha systems. *ApJ*, 378:471.
- Charlot, S. and Fall, S. M. (1993). Lyman-alpha emission from galaxies. *ApJ*, 415:580.
- Charlot, S. and Longhetti, M. (2001). Nebular emission from star-forming galaxies. *MNRAS*, 323:887.
- Chen, W. L. and Neufeld, D. A. (1994).  $Ly\alpha$  emission and absorption features in the spectra of galaxies. *ApJ*, 432:567.
- Collins, C. A., Parkes, I. M., and Joseph, R. D. (1996). Limits on  $H\alpha$  emission from young galaxies. *MNRAS*, 282:903.
- Courteau, S. (1997). Optical rotation curves and linewidths for Tully-Fisher applications. *AJ*, 114:2402.
- Cowie, L. L. and Hu, E. M. (1998). High- $z$   $Ly\alpha$  emitters. I. A blank-field search for objects near redshift  $z = 3.4$  in and around the Hubble Deep Field and the Hawaii deep field SSA 22. *ApJ*, 115:1319.
- Djorgovski, S. (1992). On the observability of primeval galaxies. In de Carvalho, R. R., editor, *Cosmology and large-scale structure in the universe*, volume 24 of *ASP Conference Series*, page 73.
- Gallego, J., Zamorano, J., Aragón-Salamanca, A., and Rego, M. (1995). The current star formation rate of the local universe. *ApJ*, 455:L1.
- Glazebrook, K., Blake, C., Economou, F., Lilly, S., and Colless, M. (1999). Measurement of the star formation rate from  $H\alpha$  in field galaxies at  $z = 1$ . *MNRAS*, 306:843.

- Gronwall, C. (1999). The star formation rate density of the local universe from the KPNO International Spectroscopic Survey. In Holt, S. and Smith, E., editors, *After the dark ages: when galaxies were young (the universe at  $2 < z < 5$ )*, page 335. AIP Press.
- Haarsma, D. B., Partridge, R. B., Windhorst, R. A., and Richards, E. A. (2000). Faint radio sources and star formation history. *ApJ*, 544:641.
- Hogg, D. W. (2001). A meta-analysis of cosmic star formation history. astro-ph/0105280.
- Hopkins, A. M., Connolly, A. J., and Szalay, A. S. (2000). Star formation in galaxies between redshifts of 0.7 and 1.8. *AJ*, 120:2843.
- Hu, E. M., Cowie, L. L., and McMahon, R. G. (1998). The density of Lyman alpha emitters at very high redshift. *ApJ*, 502:L99.
- Hu, E. M. and McMahon, R. G. (1996). Detection of Lyman- $\alpha$  emitting galaxies at redshift  $z = 4.55$ . *Nat*, 382:281.
- Hughes, D. H., Serjeant, S., Dunlop, J., Rowan-Robinson, M., Blain, A., Mann, R. G., Ivison, R., Peacock, J., Efstathiou, A., gear, W., Oliver, S., Lawrence, A., and Longair, M. (1998). High-redshift star formation in the Hubble Deep Field revealed by a submillimetre-wavelength survey. *Nat*, 394:241.
- Ivison, R. J., Smail, I., Barger, A. J., Kneib, J. ., Blain, A. W., Owen, F. N., Kerr, T. H., and Cowie, L. L. (2000). The diversity of SCUBA-selected galaxies. *MNRAS*, 315:209.
- Jones, D. H. and Bland-Hawthorn, J. (2001). The Taurus Tunable Filter field galaxy survey: sample selection and narrowband number counts. *ApJ*, 550:593.
- Kennicutt, R. C. (1983). The rate of star formation in normal disk galaxies. *ApJ*, 272:54.
- Kennicutt, R. C. (1998). Star formation in galaxies along the Hubble sequence. *ARA&A*, 36:189.
- Kudritzki, R. P., Méndez, R. H., Feldmeier, J. J., Ciardullo, R., Jacoby, G. H., Freeman, K. C., Arnaboldi, M., Capaccioli, M., Gerhard, O., and Ford, H. C. (2000). Discovery of nine Ly $\alpha$  emitters at redshift  $z \sim 3.1$  using narrowband imaging and VLT spectroscopy. *ApJ*, 536:19.
- Lilly, S. J., Lefèvre, O., Hammer, F., and Crampton, D. (1996). The Canada-France redshift survey: the luminosity density and star formation history of the universe to  $z \sim 1$ . *ApJ*, 460:L1.
- Madau, P., Ferguson, H. C., Dickinson, M. E., Giavalisco, M., Steidel, C. C., and Fruchter, A. (1996). High-redshift galaxies in the Hubble Deep Field: colour selection and star formation history to  $z \sim 4$ . *MNRAS*, 283:1388.
- Manning, C., Stern, D., Spinrad, H., and Bunker, A. J. (2000). A serendipitous search for high-redshift Ly $\alpha$  emission: two primeval galaxy candidates at  $z \sim 3$ . *ApJ*, 537:65.
- Mannucci, F. and Beckwith, S. V. W. (1995). Infrared line emission from high redshift galaxies. I. Calculations. *ApJ*, 442:569.
- Mannucci, F., Thompson, D., Beckwith, S. V. W., and Williger, G. M. (1998). Infrared emission-line galaxies associated with damped Lyman alpha and strong metal absorber redshifts. *ApJ*, 501:L11.
- McCarthy, P. J., Yan, L., Freudling, W., Teplitz, H. I., Maluluth, E. M., Weymann, R. J., Malkan, M. A., Fosbury, R. A. E., Gardner, J. P., Storrie-Lombardi, L. J., Thompson, R. I., Williams, R. E., and Heap, S. R. (1999). Emission line galaxies from the NICMOS/Hubble Space Telescope grism parallel survey. *ApJ*, 520:548.

- Mo, H. J., Mao, S., and White, S. D. M. (1998). The formation of galactic discs. *MNRAS*, 295:319.
- Moorwood, A. F. M., van der Werf, P. P., Cuby, J.-G., and Oliva, E. (2000). H $\alpha$  emitting galaxies and the cosmic star formation rate at  $z \simeq 2.2$ . *A&A*, 362:9.
- Pahre, M. A. and Djorgovski, S. G. (1995). A near infrared search for line emission from protogalaxies using the W. M. Keck telescope. *ApJ*, 449:L1.
- Pettini, M., Kellogg, M., Steidel, C. C., Dickinson, M., Adelberger, K. L., and Giavalisco, M. (1998). Infrared observations of nebular emission lines from galaxies at  $z \approx 3$ . *ApJ*, 508:539.
- Rhoads, J. E., Malhotra, S., Dey, A., Stern, D., Spinrad, H., and Jannuzi, B. T. (2000). First results from the Large-Area Lyman Alpha survey. *ApJ*, 545:L85.
- Schechter, P. (1976). An analytic expression for the luminosity function for galaxies. *ApJ*, 203:297.
- Silk, J. (1997). Feedback, disk self-regulation, and galaxy formation. *ApJ*, 481:703.
- Simard, L. and Pritchett, C. J. (1998). Internal kinematics of field galaxies at intermediate redshifts. *ApJ*, 505:96.
- Steidel, C. C., Adelberger, K. L., Giavalisco, M., Dickinson, M., and Pettini, M. (1999). Lyman break galaxies at  $z \gtrsim 4$  and the evolution of the UV luminosity density at high redshift. *ApJ*, 519:1.
- Steidel, C. C., Adelberger, K. L., Shapley, A. E., Pettini, M., Dickinson, M., and Giavalisco, M. (2000). Ly $\alpha$  imaging of a proto-cluster region at  $\langle z \rangle = 3.09$ . *ApJ*, 532:170.
- Steidel, C. C., Giavalisco, M., Pettini, M., Dickinson, M., and Adelberger, K. L. (1996). Spectroscopic confirmation of a population of normal star-forming galaxies at redshifts  $z > 3$ . *ApJ*, 462:L17.
- Stern, D., Bunker, A., Spinrad, H., and Dey, A. (2000). One-line redshifts and searches for high-redshift Ly $\alpha$  emission. *ApJ*, 537:73.
- Teplitz, H. I., Malkan, M., and McLean, I. S. (1998). An infrared search for star-forming galaxies at  $z > 2$ . *ApJ*, 506:519.
- Thompson, D., Djorgovski, S., and Beckwith, S. V. W. (1994). Searches for primeval galaxies in the near infrared. *AJ*, 107:1.
- Thompson, D., Mannucci, F., and Beckwith, S. V. W. (1996). A narrowband imaging survey for high redshift galaxies in the near infrared. *AJ*, 112:1794.
- Tresse, L. and Maddox, S. J. (1998). The H $\alpha$  luminosity function and star formation rate at  $z \approx 0.2$ . *ApJ*, 495:691.
- van der Werf, P. P., Moorwood, A. F. M., and Bremer, M. N. (2000). A large-area near-infrared emission line survey for star forming galaxies at  $z = 2.1 - 2.4$ . *A&A*, 362:509.
- Vogt, N. P., Forbes, D. A., Phillips, A. C., Gronwall, C., Faber, S. M., Illingworth, G. D., and Koo, D. C. (1996). Optical rotation curves of distant field galaxies: Keck results at redshifts to  $z \approx 1$ . *ApJ*, 465:L15.
- Vogt, N. P., Phillips, A. C., Faber, S. M., Gallego, J., Gronwall, C., Guzman, R., Illingworth, G. D., Koo, D. C., and Lowenthal, J. D. (1997). Optical rotation curves of distant field galaxies: sub- $L^*$  systems. *ApJ*, 479:L121.
- Yan, L., McCarthy, P. J., Freudling, W., Teplitz, H. I., Malumuth, E. M., Weymann, R. J., and Malkan, M. A. (1999). The H $\alpha$  luminosity function and global star formation rate from redshifts of 1-2. *ApJ*, 519:L47.